Available online at www.sciencedirect.com
SCIENCE DIRECT®
Surface Science 570 (2004) 167–177
SURFACE SCIENCE
www.elsevier.com/locate/susc

Adsorption and dissociation of CO on Fe(1 1 0) from first principles

D.E. Jiang, Emily A. Carter *

Department of Chemistry and Biochemistry, Box 951569, University of California, Los Angeles, CA 90095-1569, USA

Received 3 May 2004; accepted for publication 26 July 2004
Available online 12 August 2004

Abstract

We employ spin-polarized periodic density functional theory (DFT) to characterize CO adsorption and dissociation on the Fe(1 1 0) surface. We investigate the site preference for CO on Fe(1 1 0) at $\theta_{CO} = 0.25$ and 0.5 monolayer (ML), for different functional forms of the generalized gradient approximation (GGA) to electron exchange and correlation within DFT. At 0.25 ML, we predict the existence of a new ordered structure comparable in stability to one proposed previously. At 0.5 ML, we confirm the preference of a distorted on-top adsorption configuration suggested by experiment. The calculated heats of adsorption, CO stretching frequencies, and work function changes agree well with experiment. When dissociating from the on-top site, we predict that CO first moves off the on-top site and then goes through a lying-down transition state with a barrier of 1.52 eV. Diffusion of CO on Fe(1 1 0) from the on-top site to the long-bridge site is predicted to have a very small barrier of ~0.1 eV. Dissociation of CO from the long-bridge site goes through the same transition state as from the on-top site, but the former has a slightly lower barrier. After dissociation, O atoms remain on the surface while C atoms are embedded into Fe(1 1 0), indicating C atoms may readily diffuse into Fe(1 1 0).

Keywords: Density functional calculations; Chemisorption; Iron; Carbon monoxide

1. Introduction

The interaction between carbon monoxide and transition metal surfaces has been the subject of many investigations. Activation of CO by transition metals is an important step in many industrial processes such as car exhaust catalysis and Fischer–Tropsch synthesis. Fe is used as a catalyst in the Fischer–Tropsch process [1] due to its high ratio of activity to price. On the negative side, CO can attack steel and cause carburization [2]. In particular, CO can dissociate on a steel surface

* Corresponding author. Tel.: +1 310 206 5118; fax: +1 310 267 0319.
E-mail address: eac@chem.ucla.edu (E.A. Carter).

0039-6028/$ - see front matter © 2004 Elsevier B.V. All rights reserved.
doi:10.1016/j.susc.2004.07.035

and carbon atoms may diffuse into steel and form carbides.

Various experimental techniques have been used to characterize CO adsorption and dissociation on low-index surfaces of Fe. It has been shown that at low temperatures (room temperature or below), CO is molecularly adsorbed on Fe(1 1 0). At higher temperatures (above 380 K), decomposition takes place [3–5]. In 1981, Erley studied CO adsorption on Fe(1 1 0) using low energy electron diffraction (LEED) and high resolution electron energy loss spectroscopy (HREELS) at 120 K [6]. Fig. 1 displays four high-symmetry sites on Fe(1 1 0): the long-bridge (LB), the quasi threefold (TF), the short-bridge (SB), and the on-top (OT) sites. Erley proposed an upright OT adsorption of CO at 0.25 ML and a tilted and displaced OT adsorption at 0.5 ML.

Early semiempirical electronic structure cluster calculations (using a modified tight-binding method) [7] predicted that CO prefers the TF site at low coverage, in disagreement with experiment. A recent density functional theory (DFT) study by Stibor et al. [8] confirmed the OT adsorption of CO on Fe(1 1 0) at 0.25 ML. However, they found a displaced long-bridge (LB) site to be most stable for 0.5 ML, in disagreement with experiment. In their DFT study, the authors used the PW91 form [9] of the generalized-gradient approximation (GGA) to electron exchange and correlation. They hinted that the disagreement with experiment may be due to that particular choice of exchange-correlation functional, which is known to favor high-coordination sites [10]. Some exchange-correlation functionals have been shown to improve upon PW91 predictions. Recently, Kurth et al. tested nine exchange-correlation functionals for various systems, including atoms, molecules, surfaces, and bulk solids [11]. They found that the PKZB form [12] of the meta-GGA functional significantly improves upon PBE [13], a simplified version of PW91. Here we explore whether PKZB may be able to predict the correct site preference of CO on Fe(1 1 0).

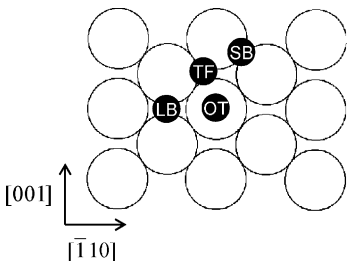

Fig. 1. High-symmetry adsorption sites on Fe(1 1 0): OT = on-top, SB = short bridge, LB = long bridge, and TF = quasi threefold.

In this work, we examine CO adsorption on Fe(1 1 0) at 0.25 ML, where we propose a new stable ordered structure, and at 0.50 ML, where we consider the possibility of a distorted OT adsorption site configuration. We test different GGA functionals to see which one yields the correct OT site preference at 0.5 ML. We compare with experiment for the CO heats of adsorption, vibrational frequencies, and work function changes. Lastly, we characterize CO dissociation pathways and barriers on Fe(1 1 0).

The paper is organized as follows. In Section 2, we present the theoretical method employed. Results for CO adsorption at 0.25 and 0.5 ML are presented in Sections 3.1 and 3.2, respectively. We then show the results for CO dissociation in Section 3.3. We discuss a likely reason for the need to tilt CO molecules at 0.50 ML on Fe(1 1 0) and the performance of several GGAs for predicting the site preference of CO on Fe(1 1 0) in Section 4. We summarize and conclude in Section 5.

2. Theoretical method

We performed first principles calculations based on spin-polarized density functional theory (DFT) [14,15]. The Vienna Ab Initio Simulation Package (VASP) [16,17] is used to solve the Kohn-Sham equations with periodic boundary conditions and a plane-wave basis set. Here we employ Blöchl's all-electron projector augmented wave (PAW) method [18] as implemented by Kresse and Joubert [19]. For the treatment of electron exchange and correlation, we use the generalized gradient approximation (GGA) of PBE and RPBE. RPBE slightly modifies PBE and has been shown to produce better adsorption energetics [10]. We also explore use of the PKZB form of the meta-GGA,

where the current VASP implementation is in the form of an a posteriori correction to PBE. Since PBE is known to be reliable for geometry optimization [20], we optimize all the structures with PBE and perform single-point calculations with RPBE and PKZB for the PBE-optimized structures.

We use a kinetic energy cutoff of 400 eV for all the calculations; this converges the total energy of, e.g., ferromagnetic (FM) bcc Fe to within 2 meV/atom. The Monkhorst–Pack scheme [21] is used for the k-point sampling. Using a $15\times15\times15$ k-mesh, we obtain an equilibrium lattice constant ($a_0 = 2.83$ Å), bulk modulus ($B = 174$ GPa), and local magnetic moment ($M = 2.20\mu_B$) for ferromagnetic bcc Fe. The results agree very well with previous PAW–GGA calculations and experiment ($a_0 = 2.86$ Å, $B = 168$ GPa, $M = 2.22\mu_B$) [22]. Placing a CO molecule in a 10 Å cubic box, we obtain its equilibrium bond length ($R_e = 1.14$ Å), bond dissociation energy ($D_e = 11.5$ eV; with respect to ^{3}P atomic carbon and ^{3}P atomic oxygen separately calculated in the same size cubic box), and harmonic vibrational frequency ($\omega_e = 2158$ cm^{-1}). The agreement with experiment is also quite good ($R_e = 1.13$ Å, $D_e = 11.2$ eV, $\omega_e = 2170$ cm^{-1}) [23].

Fe(1 1 0) is the closest-packed surface of bcc Fe and is basically bulk-terminated, with very little relaxation and no reconstruction [24]. To model the surface, we use a slab with seven layers, which we showed previously is sufficiently thick [24]. We put adsorbates on one side of the slab; this produces a dipole due to the charge rearrangement on the surface caused by adsorption. We apply an a posteriori dipole correction in the direction of surface normal; the correction to the energy is ~0.08 eV per CO.

The surface cells used for our study are shown in Fig. 2. We use a converged [24] k-mesh of $6\times8\times1$ for the rectangular cell and $7\times7\times1$ for the rhombic cell. The rectangular cell is used to study the c(2 × 4) and p(1 × 2) structures and the rhombic cell is used to study the p(2 × 2) structure. The c(2 × 4) and p(1 × 2) structures are shown in Fig. 3 and explained in the next section. Instead of using a cell shown in Fig. 3(a) to simulate the c(2 × 4) or the p(1 × 2) structure, we use the rectangle in Fig. 2, since it is a primitive cell for those two adsorption structures.

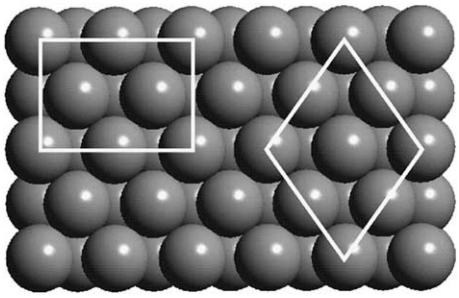

Fig. 2. Surface cells used for calculations. Rectangle for the c(2 × 4) and p(1 × 2) structures and rhombus for the p(2 × 2) structure.

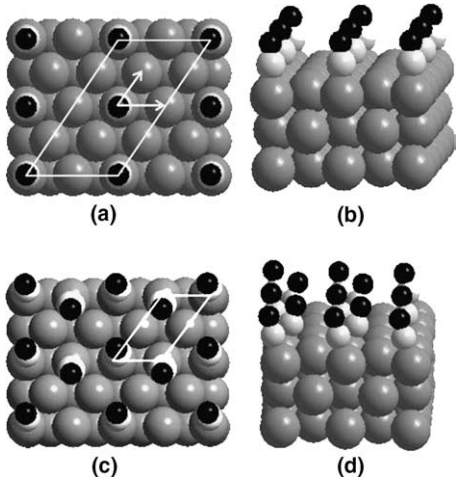

Fig. 3. Structures of CO/Fe(1 1 0) from experiment. c(2 × 4) for 0.25 ML: (a) top view and (b) side view. Distorted p(1 × 2) for 0.5 ML: (c) top view and (d) side view. Surface primitive cell vectors used to name these structures are shown in (a) and are the same for both c(2 × 4) and p(1 × 2) structures. Fe atoms are in grey, C white, and O black. The same grey scale convention is used in all subsequent figures.

Only the top three layers of the seven substrate layers are allowed to relax, together with the adsorbate layer. The bottom four layers are kept fixed in bulk positions to represent the semi-infinite bulk crystal beneath the surface. (Allowing the fourth layer of the substrate to relax only changes the total energy of the slab by ~5 meV.)

When the maximum force acting on each atom of the slab drops below 0.01 eV/Å, the structural relaxation is stopped.

The climbing image nudged elastic band (CI-NEB) method [25,26] is used to locate the minimum energy paths (MEPs) and the transition states for CO diffusion and dissociation on Fe(1 1 0). The NEB method is a reliable way to find the MEP, when the initial and final states of a process are known. An interpolated chain of configurations (images) between the initial and final positions are connected by springs and relaxed simultaneously to the MEP. With the climbing image scheme, the highest-energy image climbs uphill to the saddle point. We use the CI-NEB method to obtain the barrier for CO diffusion and dissociation on Fe(1 1 0) with the rhombic cell (see Fig. 2). However, a smaller k-mesh of $5 \times 5 \times 1$ is employed to reduce computational cost, which is estimated to change the barrier by ~0.02 eV (based on single point energy calculations at the transition state structure using a $7 \times 7 \times 1$ k-mesh). We use a force tolerance of 0.02 eV/Å for the transition state search.

The work function is obtained from the difference between the vacuum energy level (given as the value where the electrostatic potential is constant in the middle of the vacuum region) and the Fermi level. Vibrational frequencies for CO on Fe(1 1 0) are determined by diagonalizing a finite difference construction of the Hessian matrix with displacements of 0.02 Å (only allowing C and O atoms to move).

Unless noted otherwise, calculations are reported for the PBE–GGA functional only.

3. Results

3.1. Adsorption at 0.25 ML

LEED and HREELS [6] suggested a c(2 × 4) ordered structure of CO on Fe(1 1 0) at 0.25 ML coverage, as shown in Fig. 3(a) and (b). CO adsorbs on-top of Fe with the CO bond upright. With the PBE form of GGA, we explored the OT, SB, TF, and LB sites of CO on Fe(1 1 0). We found the CO bond length and the C-surface distance in the relaxed structure in very good agreement with previous PW91 results [8]. This is to be expected, since PBE is just a simplified version of PW91. We display the adsorption energies in Table 1. At 0.25 ML, PBE predicts that CO slightly prefers the OT site over the LB site, which agrees with experiment and previous PW91 predictions. The TF site is not stable, since CO relaxes to either the OT or LB site when initially put at the TF site. Our PBE adsorption energies are systematically smaller than the previous PW91 ones; this may be due to the dipole correction we use, since

Table 1
Adsorption energies ($E_{ad} = E_{Fe\text{-}slab} + E_{CO} - E_{CO/Fe\text{-}slab}$) in eV of CO at different sites on Fe(1 1 0) with different functionals

Site	PW91[a]	PBE	RPBE	PKZB
c(2 × 4): $\theta = 0.25$ ML				
OT (min)[b]	1.95	1.88	1.58	1.67
LB (min)	1.91	1.80	1.43	1.51
SB (hos)[b]	1.70	1.63	1.28	1.33
p(1 × 2): $\theta = 0.50$ ML				
OT (ts)[b]	1.81	1.66	1.32	1.46
LB (ts)	1.84	1.68	1.29	1.40
SB (hos)	1.56	1.40	1.02	1.08
Distorted OT (min)	–	1.69	1.34	1.50
Displaced LB (min)	1.86	1.72	1.34	1.38
Experiment[c]		1.24		

[a] Ref. [8].
[b] min = minimum, ts = transition state, hos = higher order saddle point.
[c] Obtained for coverages between $\theta = 0.12$ and 0.25 ML, Ref. [5].

our PBE results without a dipole correction match very well the previous PW91 results. Table 1 also shows that RPBE and the PKZB meta-GGA give the same stability trend as PBE for $\theta_{CO} = 0.25$ ML. All of the GGA forms overestimate the binding between CO and Fe(1 1 0) compared with experiment, although RPBE and PKZB correct the overbinding of PW91 and PBE by ~15% and bring the predicted adsorption energies closer to experiment.

Normal mode analysis shows that the LB and OT sites are true minima, while the SB site is a higher order saddle point for CO adsorption on Fe(1 1 0) at 0.25 ML. The calculated CO stretching frequency for the OT site (1928 cm^{-1}) agrees well with experiment (1956 cm^{-1}) [6], which is another indication that CO adsorbs at the Fe OT site. The calculated CO stretching frequency for the LB site is 1690 cm^{-1}, indicating a lower CO bond order at this site compared to the OT site. HREELS also shows a loss at 500 cm^{-1}, which is assigned as the carbon-surface stretching mode; our calculation produces a frequency of 438 cm^{-1} for this mode, for CO in the OT site.

We also explored another ordered structure for 0.25 ML, the $p(2\times2)$ structure shown in Fig. 4. Here CO also prefers the OT site, as expected. Moreover, we found this $p(2\times2)$ structure is ~10 meV more stable than the $c(2\times4)$ structure for CO on the OT site, for all three GGA functional forms. Therefore, the $p(2\times2)$ structure is likely to be as stable as the $c(2\times4)$ structure. Low temperature LEED analyses may be able to distinguish between these two structures.

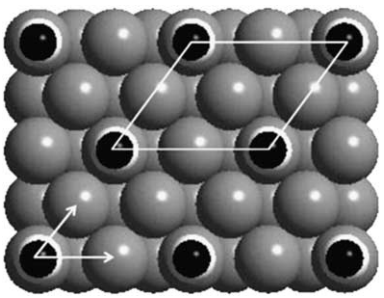

Fig. 4. The $p(2\times2)$ structure of CO adsorption on Fe(1 1 0) at 0.25 ML.

3.2. Adsorption at 0.5 ML

At 0.5 ML, LEED and HREELS data indicate that CO adsorbs on Fe(1 1 0) in a "distorted" $p(1\times2)$ configuration, as shown in Fig. 3(c) and (d) [6]. In this model, it has been suggested that CO molecules are tilted and displaced off-center from the OT site by ~0.7 Å, caused probably by steric repulsion among adsorbed CO molecules. To our knowledge, this adsorption model has not been confirmed theoretically. Starting from a displaced and tilted initial configuration, we confirmed that it is indeed a local minimum and its structure is just as experiment suggested. We found that CO molecules are displaced off the OT site by ~0.5 Å and the tilt angle of CO is ~13° from the surface normal. In the previous PW91 study by Stibor et al., they found a displaced LB site to be most stable at 0.5 ML for the $p(1\times2)$ structure, in disagreement with experiment. We also found this displaced LB site, and in our relaxed structure CO molecules are slightly displaced (~0.003 Å) off the center of the LB site towards the TF site. From the adsorption energies at 0.50 ML (Table 1), we can see that our PBE results give the same stability trend as PW91, while RPBE predicts that OT, distorted OT, LB, and displaced LB are almost degenerate. What is surprising is that PKZB correctly predicts that CO prefers the distorted OT site for the $p(1\times2)$ structure. This (perhaps fortuitous) agreement may indicate that PKZB improves upon PBE in predicting the site preference of CO on transition metal surfaces. We will discuss this further in Section 4.

Normal mode analysis shows that only the displaced LB site and the distorted OT site are true minima for CO adsorption on Fe(1 1 0) at 0.5 ML. HREELS shows that the CO stretching frequency increases from 1948 cm^{-1} at 0.25 ML for the $c(2\times4)$ structure to 1985 cm^{-1} at 0.5 ML for the $p(1\times2)$ structure. This blue shift can be explained by the dipole coupling of adsorbed CO molecules: intensity is shifted from the low-frequency out-of-phase mode to the higher frequency in-phase mode [27]. Our prediction of the in-phase CO stretching frequency (1966 cm^{-1}) for the distorted $p(1\times2)$ structure agrees

quite well with experiment. In the HREELS experiment by Erley, a wide loss band is observed between 360 and 444 cm^{-1} [6], which is in line with the six modes we found, ranging from 352 to 436 cm^{-1}, for the two CO molecules in the simulation supercell. Erley attributed the 360 and 444 cm^{-1} losses to frustrated rotation and carbon-surface stretching modes, respectively. We find that the vibrations at 436, 384, 368, and 352 cm^{-1} are all frustrated rotation modes and the vibrations at 398 and 396 cm^{-1} correspond to carbon-surface stretching modes. However, since these low frequency modes probably couple with surface phonons and since we did not include phonon coupling in our calculations, we do not want to overemphasize this discrepancy with experiment.

Measurements of work function changes at low temperature (100–120 K) from both Erley's and Wedler and Ruhmann's work [5,6] showed that the work function increases linearly upon CO exposure until it reaches saturation. The maximum change in work function was measured to be 0.86 eV by Erley for $\Theta_H = 0.25-0.50$ ML and 1.20 eV by Wedler and Ruhmann for $\Theta_H > 0.25$ ML. Our calculation predicts work function increases at 0.25 ML of 0.85 and 0.87 eV for the OT sites of the $c(2\times4)$ and $p(2\times2)$ structures, respectively, and 1.26 eV for the distorted OT site of the $p(1\times2)$ structure at 0.5 ML. The sign and magnitude of work function changes predicted here agree well with experiment. Given the inherent sensitivity of work function changes to charge transfer and structures of adsorbates on surfaces, the quantitative agreement between theory and experiment suggests that our predicted structures are likely to be correct.

3.3. CO dissociation on Fe(1 1 0) at 0.25 ML

Since 0.5 ML is the saturation coverage of CO on Fe(1 1 0), CO dissociation may occur more readily at 0.25 ML where there is more room for the products. We therefore focus on CO dissociation at $\Theta = 0.25$ ML. In Section 3.1, we showed that the $p(2\times2)$ structure is slightly more stable than the $c(2\times4)$ structure for 0.25 ML coverage. As a result, we examine CO dissociation in the $p(2\times2)$ structure. This choice of structure will not affect the dissociation energetics very much, since the energy difference between those two structures is only ~10 meV. In order to study CO dissociation with the climbing-image nudged elastic band (CI-NEB) method, we need to know the preferred adsorption sites for C and O atoms on Fe(1 1 0). Table 2 displays the adsorption energies of isolated C or O atoms on the high-symmetry sites of Fe(1 1 0). We see that C prefers the LB site on Fe(1 1 0), where the LB site is the only minimum, whereas both the TF and LB sites are minima for O, with the TF site ~10 meV lower in energy. At the most stable sites, C and O are 0.59 and 1.03 Å above the substrate surface, respectively. Next, we put both C and O atoms next to each other on Fe(1 1 0). In this case, O prefers the LB site over the TF site by ~0.20 eV, in order to minimize interaction with the neighboring C atom, which is still at the LB site but is embedded into the substrate surface by 0.28 Å. Interestingly, it seems that having an O atom nearby pushes the C atom into the substrate. We will discuss this further below.

Both experiment and our work show that CO prefers the OT site at 0.25 ML coverage, therefore we first examine CO dissociation from this site.

Table 2
Adsorption energies [$E_{ad} = E_{Fe\text{-}slab} + E_{x=C,O} - E_{x=C,O/Fe\text{-}slab}$] and height above surface ($d_{x=C\,or\,O}$) for isolated C or O atoms on Fe(1 1 0) at 0.25 ML

	OT	SB	LB	TF
$E_{ad,C}$ (eV)	5.46 (hos)	6.79 (ts)	7.77 (min)	Relaxed to LB
$E_{ad,O}$ (eV)	4.75 (hos)	5.80 (ts)	6.30 (min)	6.31 (min)
d_C (Å)	1.50	1.09	0.59	–
d_O (Å)	1.67	1.28	1.03	1.09

The nature of the critical point is given in parentheses (min = minimum, ts = transition state, and hos = higher order saddle point).

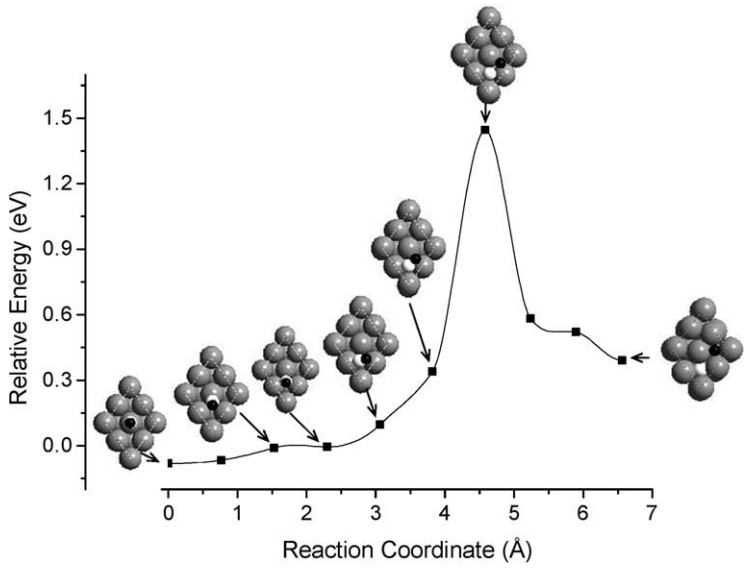

Fig. 5. DFT–GGA–PBE minimum energy path for CO dissociation on Fe(1 1 0) starting from the on-top site. Several intermediate structures along the path are shown.

The predicted MEP for CO dissociation from the OT site is displayed in Fig. 5. The CO first moves off the OT site, reorients itself, and then goes through a transition state where CO lies almost flat on the short-bridge site. The reaction is ~0.50 eV endothermic and has a barrier of 1.52 eV. At the transition state, the C–O bond is very elongated (~1.74 Å). This type of transition state is quite common for CO dissociation on transition metal surfaces [28,29]. In the final structure along the path, one can see that the C atom embeds itself into the Fe(1 1 0) surface (0.28 Å below the surface) after dissociation; this species is a likely precursor to carburization. At the final state, the O atom is ~1.0 Å above the surface, close to the value for O on Fe(1 1 0) without C (Table 2).

Although CO prefers the OT site at 0.25 ML, the C–O bond is 0.02 Å longer and the CO stretching frequency is ~240 cm^{-1} lower in the LB site than the corresponding value for the OT site. This suggests that the C–O bond could be weaker at the LB site. We find that the diffusion barrier from the OT site to the LB site is very low (~0.10 eV), so the LB site is easily accessible from the OT site. Fig. 6 displays the predicted MEP starting from the LB site as well as several structures along the dissociation path. If we compare Fig. 6 with Fig. 5, we can see that the path for the LB site is exactly the same as the later part of the path for the OT site. Due to the lower energy of the OT site, the overall dissociation barrier from the OT site is slightly (~0.10 eV) higher than from the LB site. Although there is a slight preference for diffusion followed by dissociation at the LB site, the energetics are so similar (within 0.1 eV) that we conclude that it is roughly equally likely for CO to dissociate from either the OT or the LB sites.

For CO dissociation on Fe(1 1 0) from the OT site, we obtain a dissociation barrier of 1.52 eV for the PBE functional, which is ~0.40 eV higher than that on Fe(1 0 0) [30], indicating that Fe(1 1 0) is less active towards CO. This is in agreement with experimental observation [31]. The CO dissociation barriers for the RPBE and PKZB functionals are 1.83 and 1.77 eV, respectively. The dissociation barrier is ~0.30 eV smaller for PBE (but 0.25 and 0.10 eV greater for RPBE and PKZB, respectively) than the calculated CO desorption barrier from the LB site (Table 1; here we quite reasonably assume no barrier to adsorption exists so that the adsorption energy equals the desorption barrier). As discussed earlier and

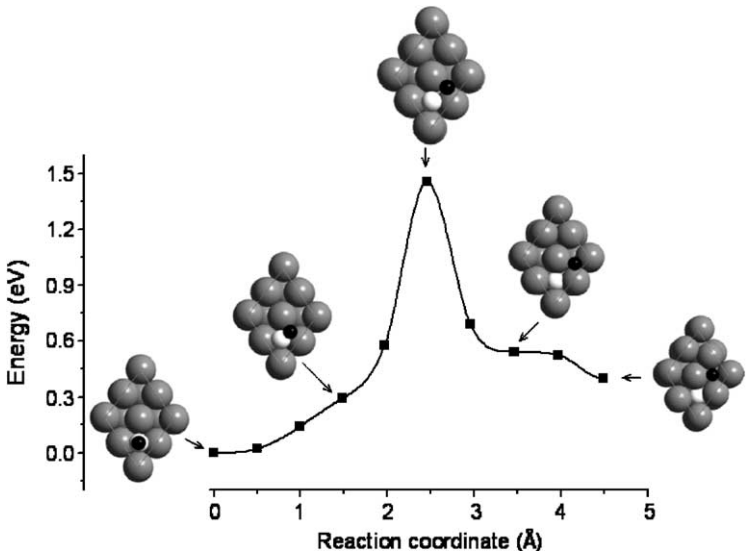

Fig. 6. DFT–GGA–PBE minimum energy path for CO dissociation on Fe(110) starting from the long-bridge site. Several intermediate structures along the path are shown.

from what previous work [24] has shown, RPBE and PKZB yield better adsorption energetics than PBE, which often overestimates the adsorption energy by >30% compared with experiment [10]. We therefore believe that comparing dissociation barriers and desorption energies for RPBE and PKZB will be more relevant to experiment. We therefore conclude that since the predicted dissociation barrier is only 0.10–0.25 eV higher than the predicted desorption energy, dissociation should compete with molecular desorption upon heating. This is indeed what has been observed in experiment [3,5]. Thermal desorption experiments [3] exhibit one peak at 400 K from molecularly adsorbed CO and another peak at ~775 K from recombinative desorption of dissociatively adsorbed CO.

4. Discussion

Our present work shows that DFT-PBE predicts a tilted state for CO on Fe(110) at 0.50 ML and DFT-PKZB also predicts this tilted state as the most stable site, consistent with LEED measurements. Here we discuss possible origins of the tilted state and the sensitivity of the results to the choice of GGA.

4.1. Tilted state of CO on transition metal surfaces at high coverage

The fact that steric repulsion causes the CO axis to tilt at higher coverages on transition metal surfaces is well established by experiments [32–36]. Surfaces on which CO tilt has been observed include Ni(110), Pd(110), Pd(100), Ru(001), Pt(112) steps, etc. Since 0.50 ML is the experimental saturation coverage of CO on Fe(110), this should be considered a quite high CO coverage for this surface. This is consistent with the fact that the surface atom density (atoms per unit area) is quite high for Fe(110), due to the small lattice parameter of bcc Fe. Indeed, 0.50 ML of CO on Fe(110) amounts to an absolute surface coverage of 0.088 CO molecule/Å^2, very similar to the absolute surface coverage of 1.0 ML of CO on Pd(110) of 0.094 CO molecule/Å^2.

When a dense layer of CO molecules are adsorbed on a metal surface, the distance between two nearest-neighbor adsorption sites available to CO can be smaller than the van der Waals diameter of CO (~3.0 Å) [6], which then forces CO molecules to tilt in order to reduce steric repulsion. For example, on Pd(110), the nearest-neighbor distance is 2.75 Å and a tilted state is observed

for the (2×1)p2mg-CO structure at 1 ML [36]. Likewise, the nearest-neighbor distance on Fe(1 1 0) is even smaller, 2.48 Å, which is too small for occupation by two aligned CO molecules. This is why half of the rows of Fe atoms on Fe(1 1 0) are not occupied by CO even at saturation coverage (0.50 ML). The distance between the next-nearest-neighbor adsorption sites for CO on Fe(1 1 0) is 2.83 Å along [0 0 1]. This distance is large enough to allow two CO molecules to occupy the two sites, but is still smaller than the van der Waals diameter of CO. So tilting of CO molecules follows.

It is clear from the above analysis that steric repulsion causes CO to tilt on Fe(1 1 0) at 0.50 ML coverage. Part of the analysis was done by Erley when he offered an explanation of the $p(2\times1)$-CO structure on Fe(1 1 0) [6]. In our case, it is fortuitous that DFT correctly captures this steric repulsion of CO on Fe(1 1 0), since the available DFT exchange-correlation functionals do not contain the essential physics required to describe van der Waals interactions properly.

4.2. Site preference predictions for CO on Fe(1 1 0): sensitivity to choice of GGA

Recently, there has been some discussion about the accuracy of current implementations of DFT for describing chemisorption [37–40]. Here we consider the origin of the success of the PKZB meta-GGA in predicting the correct site preference of CO on Fe(1 1 0). Stibor et al. [8] showed that PW91 predicts the correct site preference at 0.25 ML but the wrong one at 0.5 ML. This tendency to overbind small molecules (or atoms) in high metal coordination sites is most clearly demonstrated in the case of CO adsorption on Pt(1 1 1). Almost all experiments clearly place CO on top of a Pt atom at low coverage, while PW91 predicts the fcc-hollow site to be the most stable [37]. Various arguments have been offered to explain this discrepancy. Kresse et al. [39] proposed that the error comes from the underestimated CO HOMO-LUMO gap by the DFT–GGA(PW91) functional, yielding too strong an interaction of the LUMO of CO with the metal substrate at the hollow site. Using of a semi-empirical DFT method such as GGA + U or B3LYP, which can artificially increase the HOMO-LUMO gap, yields the correct site preference of CO on Pt(1 1 1) [39].

Another explanation of DFT–GGA's incorrect prediction of site preference is offered by Grinberg et al. [38]. They argue that the error is due to the GGA treating different bond orders with varying accuracy. Since the CO bond has a different order at the on-top adsorption site compared to the hollow adsorption (as inferred from CO frequency trends), DFT–GGA may describe them with different degrees of accuracy. Thus, Grinberg et al. proposed that the advantage of error cancellation is lost and the wrong site preference is produced. They then suggested that the PKZB meta-GGA functional may predict the right site preference, due to its excellent performance for both small molecules and extended systems (surfaces and solids), as demonstrated by Kurth et al. [11]. Just as Grinberg et al. suggested, we did find that the PKZB meta-GGA functional predicts the correct site preference of CO on Fe(1 1 0). The VASP code used here only supports non-self-consistent DFT calculations for the PKZB functional using self-consistent densities from the PBE functional. Therefore the HOMO-LUMO gap of CO remains that predicted by PBE (too low), even though the total energy changes. So Kresse et al.'s analysis does not appear to hold in this case. The "gap" problem may be not as big an issue in the CO/Fe(1 1 0) system as in the CO/Pt(1 1 1) system. This is supported by the fact that DFT–GGA(PBE) does predict the right site preference of CO on Fe(1 1 0) at 0.25 ML. It should be noted that there is one empirical parameter in the PKZB meta-GGA functional, which is obtained by fitting experimental data. Recently, Tao et al. developed a new functional form (TPSS) [41] of meta-GGA that eliminates that empirical parameter from PKZB. However, TPSS has not been implemented in the version of the code used here, so we could not test it. We caution that the non-self-consistent way VASP calculates the PKZB energy might be not reliable and the predicted correct site preference from the PKZB functional might be fortuitous.

Although the RPBE functional gives the best prediction of the adsorption energy of CO on Fe(1 1 0), it predicts that the OT, distorted OT,

LB, and displaced LB sites are almost degenerate. RPBE and previous revPBE [42] predictions of chemisorption energies are superior, due to their excellent performance on atomic total energies and molecular atomization energies. However, they worsen the descriptions of bulk crystals and surfaces compared with PBE [10,20]. This may account for the fact that RPBE does not predict the right site preference of CO on Fe(1 1 0) at 0.5 ML.

5. Summary and conclusions

Employing first principles PAW–DFT–GGA techniques, we have studied CO adsorption, diffusion, and dissociation on Fe(1 1 0). In agreement with experiment and previous theory, we find that CO adsorbs in a upright fashion and the on-top (OT) site is preferred over the long-bridge (LB) and short-bridge (SB) sites for 0.25 ML coverage. We also find a new $p(2\times2)$ structure of CO on Fe(1 1 0) at 0.25 ML, which is different from, but predicted to be as stable as, the $c(2\times4)$ structure suggested by experiment. We confirm the stability of the distorted OT $p(1\times2)$ structure at 0.5 ML proposed from experiment. Here the CO molecule is displaced off the on-top site by 0.5 Å and the CO bond is tilted $\sim13°$ with respect to the surface normal. Steric repulsion is likely the reason CO molecules tilt in an alternating fashion. While all GGAs yield the correct site preference at 0.25 ML, only the PKZB meta-GGA predicts the correct site preference of CO on Fe(1 1 0) for both 0.25 and 0.5 ML. We predict CO stretching frequencies of 1928 and 1966 cm^{-1} and work function changes of ~0.86 and ~1.24 eV for the most stable site at 0.25 and 0.5 ML, respectively, in good agreement with experiment.

We have examined CO dissociation on Fe(1 1 0) at 0.25 ML. Starting from the most stable OT site, CO dissociation on Fe(1 1 0) is endothermic by ~0.5 eV and has a barrier of 1.52 eV. CO first moves off the OT site and then dissociates via a transition state where CO is lying down on the SB site. We predict that the CO diffusion barrier across the Fe(1 1 0) surface is small (~0.1 eV from the OT site to the LB site). Since the LB site is easily accessible from the OT site, we also investigated CO dissociation at the LB site. We find that CO dissociates from the LB site via the same transition state as from the OT site but has a slightly lower barrier, because the LB site is slightly higher in energy that the OT site.

The high barrier (1.52 eV from the OT site) of CO dissociation on Fe(1 1 0) is consistent with the fact that the decomposition of CO on Fe(1 1 0) is only observed at high temperatures (above room temperature). CO dissociation is found to be competitive with molecular desorption, thereby providing the means to produce adsorbed carbon and oxygen atoms on the surface. After dissociation, O atoms remain on the surface while C atoms burrow into Fe(1 1 0), presumably as the initial step toward carburization of Fe.

Acknowledgments

We are grateful to the Army Research Office for support of this work. We thank the Maui High Performance Computing Center and the NAVO Major Shared Resources Center for CPU time.

References

[1] R.B. Anderson, The Fischer–Tropsch Synthesis, Academic Press, Orlando, FL, 1984.
[2] H.J. Grabke, Carburization: A High Temperature Corrosion Phenomenon, Elsevier, Amsterdam, The Netherlands, 1998.
[3] L. Gonzalez, R. Miranda, S. Ferrer, Surf. Sci. 119 (1982) 61.
[4] G. Wedler, H. Ruhmann, Surf. Sci. 121 (1982) 464.
[5] G. Wedler, R. Ruhmann, Appl. Surf. Sci. 14 (1983) 137.
[6] W. Erley, J. Vac. Sci. Technol. 18 (1981) 472.
[7] S.P. Mehandru, A.B. Anderson, Surf. Sci. 201 (1988) 345.
[8] A. Stibor, G. Kresse, A. Eichler, J. Hafner, Surf. Sci. 507–510 (2002) 99.
[9] J.P. Perdew, J.A. Chevary, S.H. Vosko, K.A. Jackson, M.R. Pederson, D.J. Singh, C. Fiolhais, Phys. Rev. B 46 (1992) 6671.
[10] B. Hammer, L.B. Hansen, J.K. Nørskov, Phys. Rev. B 59 (1999) 7413.
[11] S. Kurth, J.P. Perdew, P. Blaha, Int. J. Quantum Chem. 75 (1999) 889.
[12] J.P. Perdew, S. Kurth, A. Zupan, P. Blaha, Phys. Rev. Lett. 82 (1999) 2544.
[13] J.P. Perdew, K. Burke, M. Ernzerhof, Phys. Rev. Lett. 77 (1996) 3865.

[14] P. Hohenberg, W. Kohn, Phys. Rev. 136 (1964) B864.
[15] W. Kohn, L.J. Sham, Phys. Rev. 140 (1965) A1133.
[16] G. Kresse, J. Furthmüller, Phys. Rev. B 54 (1996) 11169.
[17] G. Kresse, J. Furthmüller, Comput. Mater. Sci. 6 (1996) 15.
[18] P.E. Blöchl, Phys. Rev. B 50 (1994) 17953.
[19] G. Kresse, D. Joubert, Phys. Rev. B 59 (1999) 1758.
[20] J.P. Perdew, K. Burke, M. Ernzerhof, Phys. Rev. Lett. 80 (1998) 891.
[21] H.J. Monkhorst, J.D. Pack, Phys. Rev. B 13 (1976) 5188.
[22] D.E. Jiang, E.A. Carter, Phys. Rev. B 67 (2003) 214103.
[23] K.P. Huber, G. Herzberg, Molecular Spectra and Molecular Structure, 4: Constants of Diatomic Molecules, Van Norstrand Reinhold Co., New York, 1979.
[24] D.E. Jiang, E.A. Carter, Surf. Sci. 547 (2003) 85.
[25] H. Jónsson, G. Mills, K.W. Jacobsen, in: B.J. Berne, G. Ciccotti, D.F. Coker (Eds.), Classical and Quantum Dynamics in Condensed Phase Simulations, World Scientific, Singapore, 1998, p. 385.
[26] G. Henkelman, B.P. Uberuaga, H. Jónsson, J. Chem. Phys. 113 (2000) 9901.
[27] P. Hollins, J. Pritchard, Prog. Surf. Sci. 19 (1985) 275.
[28] J.K. Nørskov et al., J. Catal. 209 (2002) 275.
[29] J. Greeley, J.K. Nørskov, M. Mavrikakis, Annu. Rev. Phys. Chem. 53 (2002) 319.
[30] D.C. Sorescu, D.L. Thompson, M.M. Hurley, C.F. Chabalowski, Phys. Rev. B 66 (2002) 035416.
[31] G.A. Somorjai, Introduction to Surface Chemistry and Catalysis, Wiley, New York, 1994.
[32] P. Uvdal, P.A. Karlsson, C. Nyberg, S. Andersson, N.V. Richardson, Surf. Sci. 202 (1988) 167.
[33] J. Lee, J. Arias, C. Hanrahan, R. Martin, H. Metiu, C. Klauber, M.D. Alvey, J.T. Yates Jr., Surf. Sci. 159 (1985) L460.
[34] W. Riedl, D. Menzel, Surf. Sci. 163 (1985) 39.
[35] M.A. Henderson, A. Szabo, J.T. Yates Jr., Chem. Phys. Lett. 168 (1990) 51.
[36] H. Kato, M. Kawai, J. Yoshinobu, Phys. Rev. Lett. 82 (1999) 1899.
[37] P.J. Feibelman, B. Hammer, J.K. Norskov, F. Wagner, M. Scheffler, R. Stumpf, R. Watwe, J. Dumesic, J. Phys. Chem. B 105 (2001) 4018.
[38] I. Grinberg, Y. Yourdshahyan, A.M. Rappe, J. Chem. Phys. 117 (2002) 2264.
[39] G. Kresse, A. Gil, P. Sautet, Phys. Rev. B 68 (2003).
[40] R.A. Olsen, P.H.T. Philipsen, E.J. Baerends, J. Chem. Phys. 119 (2003) 4522.
[41] J.M. Tao, J.P. Perdew, V.N. Staroverov, G.E. Scuseria, Phys. Rev. Lett. 91 (2003).
[42] Y.K. Zhang, W.T. Yang, Phys. Rev. Lett. 80 (1998) 890.